# DETERMINATION OF DISCHARGE COEFFICIENTS OF SONIC NOZZLES OBTAINING LOW UNCERTAINTY WITHOUT KNOWLEDGE OF THROAT DIAMETER.

Authors: Bodo Mickan, Rainer Kramer, Petra Kiesewetter, Dietrich Dopheide

Physikalisch-Technische Bundesanstalt
Bundesallee 100
D-38116 Braunschweig
Germany
e-mail: bodo.mickan@ptb.de
phone: ++49 531 592 1331
fax: ++49 531 592 69 1331

The paper presents a new approach for the determination of discharge coefficients of sonic nozzles. Innovating the conventional way, where the knowledge of throat diameter is always necessary, the new approach utilises a special mathematical characteristic of the equation $c_D = a + b \cdot Re^{-0.5}$ to figure out a relationship of the parameter $b$ as a function of the parameter $a$ and to define a new parameter $\beta$ with $b = f(a,\beta)$.

It is shown in the paper by theory as well as by experimental results, that the parameter $\beta$ can be determined only from measurements of flow rate and gas parameters without any knowledge about throat diameter.

With parameter $a$ as a parameter which is very well known with low uncertainty from past research and theoretical studies, the discharge coefficient $c_D = a + b \cdot Re^{-0.5} = a + f(a, \beta) \cdot Re^{-0.5}$ can be determined now also for very small nozzles down to a Reynolds number $Re$ = 1000 (throat diameter roughly 0.1 mm) with a very low uncertainty.

Additional to this, it is shown based on measurements of more than 300 nozzles, that the new parameter $\beta$ is related to the inner geometry of the nozzle and a sensitive indicator of the quality of manufacturing and/or the measurements.

Nomenclature

| Symbol | Meaning |
|---|---|
| $a$, $b$ | parameter of $c_D$-$Re$-relation (Eq. 2); |
| $a_d$, $b_d$ | parameter of $y$-$x$-relation (Eq. 5); |
| $c_D$ | discharge coefficient |
| $c_{D,inf}$ | infinite discharge coefficient ($Re \rightarrow \infty$), equal to $a$ |
| $c^*$ | Critical flow factor |
| $d$ | geometric throat diameter |
| $G$ | Geropp-factor (Eq. 21) |
| $H_l$ | coefficient of Hall´s equation of $c_{D,inf}$ (Eq. 16) |
| $p_0$ | gas pressure at nozzle entrance (stagnation conditions) |
| $q_m$ | mass flow rate |
| $R$ | curvature radius of nozzle inlet, given in units of throat diameter $d$ (e.g. $R$ =2 means $R = 2 \cdot d$) |
| $Re$ | Reynolds number |
| $R_{gas}$ | gas constant |
| $T_0$ | gas temperature at nozzle entrance (stagnation conditions) |
| $x$ | linearised flow scale (Eq. 3) |
| $y$ | effective (hydraulic) area (Eq. 3) |
| $\beta$ | $c_D$-gradient (Eq. 11) |
| $\delta^*$ | Boundary layer thickness (mass flow defect) |
| $\eta$ | dynamic viscosity |
| $\kappa$ | isentropic exponent (= 1,4 for air) |

Introduction

In the last years the number of sonic nozzles applied as long term stable working standards in calibration facilities of state approved laboratories and in the industry has been increased more and more. In the PTB a few hundred nozzles were calibrated in the last years and the quality control of these calibrations became more and more important. In the following we discuss results of calibrations of 364 nozzles calibrated with air near to atmospheric conditions[1]. The size of nozzles are hereby from throat diameters of 0,1 mm (i.e. about 5 l/h volume flow rate with atmospheric air at the nozzle entrance) upwards to 10 mm. All of them were specified as circular-arc nozzles according ISO 9300 with curvature radius $R = 2d$ (in the following always called $R = 2$).

To control the quality of nozzle calibration it would be the most natural approach to compare the discharge coefficient of a nozzle with the best known values we have, because the discharge coefficient is a dimensionless number only depending on Reynolds number. Eq. 1 gives the definitions of both ($c_D$ and $Re$) and Eq. 2 the dependency of $c_D$ on $Re$ for the region of laminar boundary layers.

Eq. 1 $$c_D = \frac{q_m}{q_{m,theor}} = \frac{4q_m\sqrt{RT_0}}{\pi d^2 c^* p_0} \text{ and } Re = \frac{4q_m}{\pi \eta d}$$

Eq. 2 $$c_D = a - \frac{b}{\sqrt{Re}}$$

[1] It is not the intention of the paper to explain the different primary standards used for the calibrations. For this, please refer to the CMC-tables at the web sites of BIPM/CIPM and the references given there.

The parameters *a* and *b* in Eq. 2 were determined by many researchers in the last decades applying least square fits on their experimental results. Table 1 gives an overview to some of these results inclusive the values of theoretical studies.

Table 1published values of parameter *a* and *b*

| Author | *a* | *b* |
|---|---|---|
| Arnberg 73 [Arnberg 73] | 0,9974 | 3,306 |
| Arnberg 74 [Arnberg 74] | 0,9973 | 3,323 |
| Brain 77 [Brain 77] | 0,9969 | 6,245 |
| Brain 78 [Brain 78] | 0,9984 | 4,420 |
| Aschi 78/79 [Aschi 78/79] | 0,9974 | 3,312 |
| Ishibashi 94 [Ishibashi 94] | 0,9986 | 3,411 |
| Nakao [Nakao] | 1,007 | 3,195 |
| Nakao [Nakao] | 1,006 | 3,783 |
| Miralles 98 [Miralles 98] | 0,9965 | 2,673 |
| PTB 99 [PTB 99] | 0,9982 | 3,448 |
| NRLM 99 [NRLM 99] | 0,9986 | 3,447 |
| Park 2000 [Park 2000] | 0,9985 | 3,344 |
| Lavante [Lavante] (numerical by CFD) | 1 | 4 |
| Stratford 64 [Stratford 64] (theoretical) | 0,9984 | 3,032 |
| Hall/Geropp [Hall] [Geropp] (two theories combined, see Eq. 15ff) | 0,9986 | 3,516 |

As it is to be seen in table 1, the values of *a* and *b* vary in a wide range. The most recent researchers come to values for a ≈ 0,9985 and b ≈ 3,5 what is in good agreement with theoretical values coming from Hall/Geropp [Hall] [Geropp] (see also Eq. 15ff).

But in our case the greatest problem to compare an actual calibration with these results is the uncertainty of throat diameter measurement. For our smallest nozzle with $d$ = 0,1 mm an uncertainty of only 1 µm (what is unrealistic low) would lead to an uncertainty in $c_D$ – determination of 2 % ! Hence, this way is not sufficient to come to a quality control and we went to one step back. This means elimination of the throat diameter from the definitions in Eq. 1 what leads to Eq. 3.

Eq. 3 $$y = c_D d^2 = \frac{4 q_m \sqrt{R T_0}}{\pi c^* p_0} \quad \text{and} \quad x = \frac{1}{\sqrt{Re \cdot d}} = \sqrt{\frac{\pi \eta}{4 q_m}} .$$

The quantity $y$ can be interpreted here as the effective throat area and the quantity $x$ as the linearised flow scale, because the results follow a linear function in the $x$-$y$-diagram (see also Fig. 1).

Using additionally

Eq. 4 $a_d = a \cdot d^2$ and $b_d = b \cdot d^{\frac{5}{2}}$

we transform Eq. 2 into:

Eq. 5 $y = a_d - b_d x$.

For any nozzle, which is calibrated at different inlet pressures[2], we get typically a graph as it is given in Fig. 1. The single results for each nozzle can be approximated by the linear function[3] given in Eq. 5.

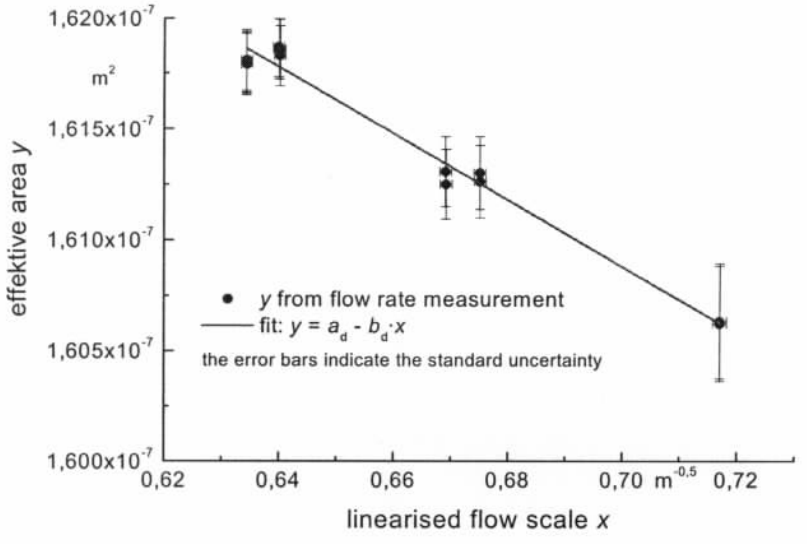


Fig. 1: Typical example of results for the effective throat area $y$ of a sonic nozzle versus scale $x$. Both, $x$ and $y$ can be determine from flow rate measurement using Eq. 3. The results can be described by a linear fit (Eq. 5) for the application of the nozzle within the range of laminar boundary layer.

It is interesting now to look to all results of $a_d$ and $b_d$ which we got from our calibrations of 364 nozzles. In Fig. 2 $b_d$ is plotted against $a_d$ and it is fascinating to see the strong correlation between both parameters.

[2] The typical values for calibrations of sonic nozzles for customers in the PTB are 1000, 900 and sometimes 800 mbar. This covers the most of the applications of our customers.

[3] It is not important for the fit that both quantities $y$ and $x$ depending on mass flow rate $q_m$. For a correct use of the uncertainties it is the most simple way to transform the fitting problem to the implicit function $z = 0 = y - a_d + b_d \cdot x$, where all uncertainties of input variables can be propagated to the variable $z$ in conformity with the GUM.

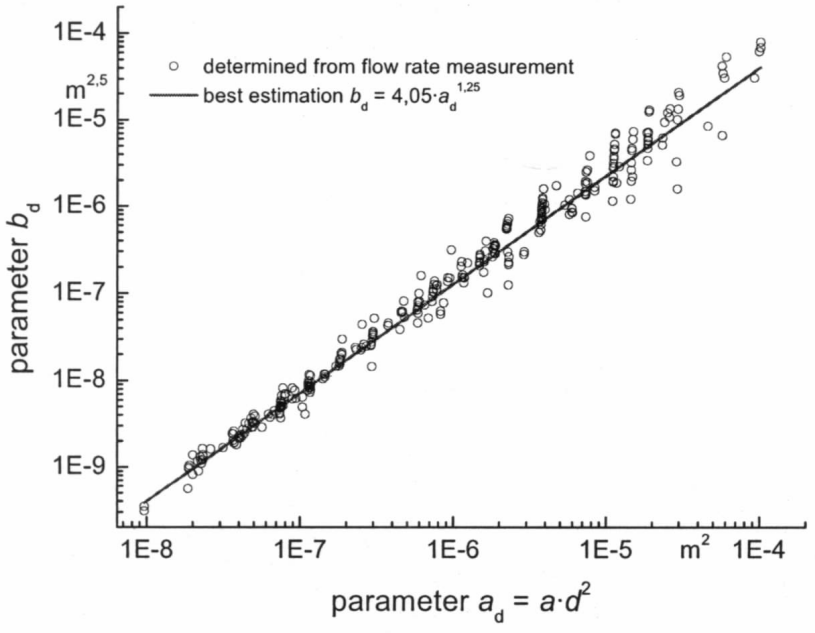


Fig. 2: Correlation between the two parameter $a_d$ and $b_d$ of linear fits (see also fig. 1) applied on results of 364 different nozzles (see also fig. 1). The set of nozzles covers throat diameters of roughly 0,1 to 10 mm.
For the relation $b_d = \beta \cdot a_d^{1,25}$ see text from Eq. 7 to Eq. 11. For explanation of the best estimation $\beta = 4{,}05$ see text and Fig. 5 + 6.

Concerning the log-scales in Fig. 2, the correlation can be obviously described by a model like

Eq. 6 $b_d = \beta \cdot a_d^{\alpha}$.

This is already a good tool for our purpose of quality control, because we could use this experimental result for a basis to decide whether a calibration is statistical significant different from the mean or not. But the question was now, if we can find some more information about the correlation between $a_d$ and $b_d$ and some relation to the physics of sonic nozzles.

The introduction of $c_D$-gradient $\beta$

In the following we want to introduce the $c_D$-gradient $\beta$ as a dimensionless constant of a sonic nozzle which can be determined without knowledge of throat diameter. For this purpose we look in detail to the mathematical behaviour of our primary relation Eq. 2 which we can transform (concerning Eq. 4) to:

Eq. 7 $$c_D = \frac{a_d}{d^2} - \frac{b_d}{d^{\frac{5}{2}}\sqrt{Re}} = C^4 a_d - C^5 b_d \frac{1}{\sqrt{Re}} \quad \text{with} \quad C = \frac{1}{\sqrt{d}}.$$

We assume now a given nozzle which has its characteristic parameters $a_d$ and $b_d$ (see also Fig. 1 and Eq. 5). Than we can look to all different curves which can be established by Eq. 7 using any value of constant $C$. In Fig. 2 three examples are shown.

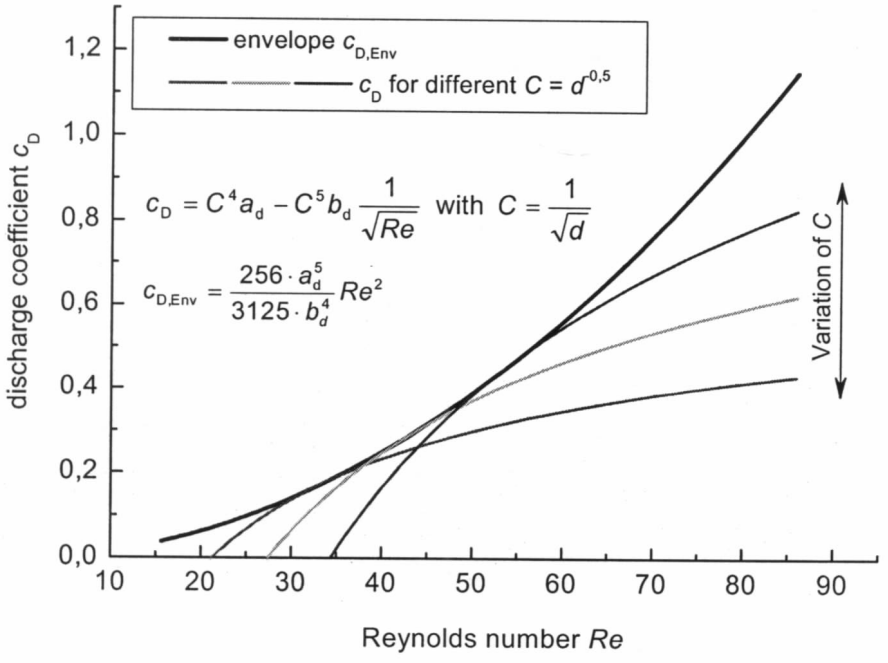


Fig. 3: Set of $c_D$-curves created by variation of constant $C = d^{0.5}$ for a given nozzles, which has its characteristic parameters $a_d$ and $b_d$ (see also Fig. 1 and Eq. 4+ Eq. 5). All possible curves have a common envelope as given by Eq. 10.
Note that the point of touching the envelope is far away from the normally used range of Reynolds number of a sonic nozzle.

As it is outlined in Fig. 2 all possible curves of $c_D$ have a common envelope. This is an interesting fact and it is helpful for us to determine the function of the envelope. It is a mathematical formalism[4] which goes out from the implicit formulation of Eq. 7:

Eq. 8 $$F(c_D, Re, C) = -c_D + C^4 a_d - C^5 \frac{b_d}{\sqrt{Re}} = 0 \cdot$$

At the points of touching the envelope is identical to the tangents of the curves, therefore the condition for the envelope is the first derivative of Eq. 8 with respect to the constant $C$:

Eq. 9 $$\frac{\partial F}{\partial C} = 4C^3 a_d - 5C^4 \frac{b_d}{\sqrt{Re}} = 0; \Rightarrow C = \frac{4 a_d \sqrt{\mathrm{Re}}}{5 b_d} \cdot$$

With this result for the constant $C$ we can transform Eq. 7 to:

Eq. 10 $$c_{D,Env} = \frac{256 \cdot a_d^5}{3125 \cdot b_d^4} Re^2 = A_{Env} Re^2 \cdot$$

The envelope is a quadratic function of Reynolds number as given by Eq. 10. The constant $A_{Env}$ is already near to our aim to find a dimensionless number characterising a given sonic nozzle. We can use $A_{Env}$ to define the new parameter "$c_D$-gradient $\beta$" (also concerning Eq. 4) with:

Eq. 11 $$\beta = \sqrt[4]{\frac{256}{3125 \cdot A_{Env}}} = \frac{b_d}{a_d^{1.25}} = \frac{b}{a^{1.25}}$$

what leads finally to

Eq. 12 $b = \beta \cdot a^{1.25}$ or $b_d = \beta \cdot a_d^{1.25}$

[4] This formalism is given in most of standard lecture books for mathematics.

Eq. 12 is the new relation between the original parameter $a$ and $b$ as well as of $a_d$ and $b_d$ (compare also Eq. 6). We can transform Eq. 2 now to

Eq. 13 $$c_D = a - \frac{\beta \cdot a^{1.25}}{\sqrt{Re}}$$

where $\beta$ (called $c_D$-gradient) is a new parameter which can be determined from flow rate measurement of a sonic nozzle without any knowledge of throat diameter. If the parameter $a$ is known from other sources of information, the $c_D$-curve of a sonic nozzle is fully determined.

Statistic of $c_D$-gradient $\beta$

Using the very helpful result of Eq. 12 we can now discuss all results of $c_D$-gradient $\beta$ for our set of 364 nozzles. The single results are shown in Fig. 4.

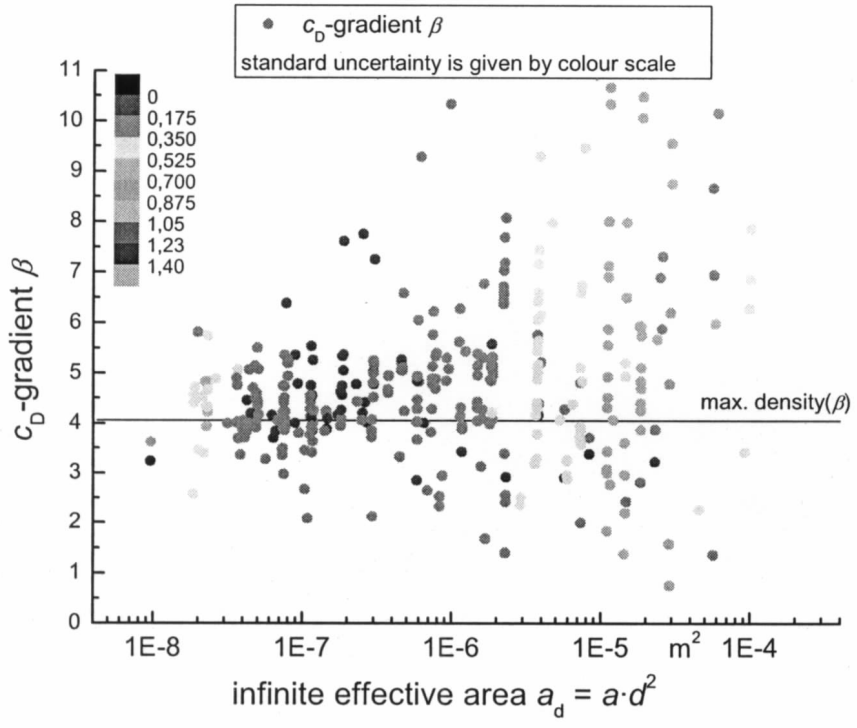


Fig. 4: Results of the $c_D$-gradient $\beta$ for 364 sonic nozzles (same set as in fig. 2). The standard uncertainties are given by the colour scale (error bars would destroy the perceptibility of the layout).
Most of the values are statistical significant different (difference is more than the quadratic sum of the expanded uncertainties), hence the scatter of data are mainly not caused by the uncertainty of measurement. For explanation of the maximum density($\beta$) see also Fig. 5 and 6.

The scatter of the $c_D$-gradient $\beta$ in Fig. 4 is large and makes the interpretation quite difficult. First we have to consider if the single values are statistical significant different or not. Concerning the uncertainties of $\beta$ (which is given in Fig. 4 by colour scale) we found most of them as significant different. That means the scatter in Fig. 4 is not caused by the uncertainty or reproducibility of measurement[5] but lies in different behaviours of the nozzles.

The next question is to ask for any representative value of $\beta$. For this purpose we establish the numerical probability density for the values of $\beta$. It is easily done by using the statistical chart of accumulated numbers versus $\beta$ (sorted by increasing values) as given in Fig. 5. On this chart the formula:

[5] The uncertainty of $\beta$ depends strongly on the covered Reynolds range. For further studies a range of $Re_{min}/Re_{max} = 0.5$ is recommended especially for higher $Re$ - numbers.

Eq. 14 $$density(\beta_i) = \frac{2 \cdot m}{\beta_{i+m} - \beta_{i-m}}$$

can be applied, what is the numerical density (first derivative). The parameter $m$ in Eq. 14 helps to smoothing the resulting curve. In our case with 364 values we choose $m = 13$ as a convenient value. The resulting density is shown in Fig. 6. The shape of such a curve is very close to a histogram but the advantage is that the curve conserves the original resolution.

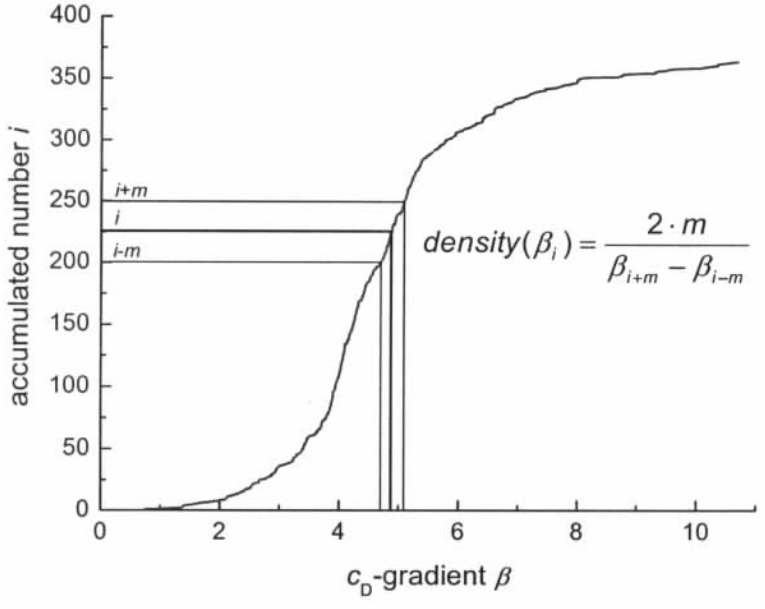


Fig. 5: Accumulated number of results of $c_D$-gradient $\beta$ (data set of Fig. 4 sorted by increasing value). This statistical chart is helpful to determine the most probably value of $\beta$ using the numeric density. The searched value is the point of highest gradient in the curve above.

In Fig. 6 can be observed one sharp maximum at $\beta = 4{,}05$ (with small side peaks) and two further peaks at $\beta = 4{,}83$ and $\beta = 5{,}14$. For further discussions they are numbered as peak 1, 2 and 3 with decreasing height. The shape of curve in Fig. 6 indicates a multipoint distribution far away from any normality or uniformity. Therefore the use of any kind of mean or median would not be helpful to characterise a representative value of $\beta$. As we consider that all nozzles calibrated here were specified according ISO 9300 with curvature radius $R = 2$, we have to realise different sets of nozzles with the same systematic effect for each peak. It is reasonable to assume that the maximum peak 1 represents the most probably value where the nozzles fit in the best way to their specifications. Therefore we choose $\beta = 4{,}05$ as the best estimation from the experiment with an expanded uncertainty of 0,15 (derived from the peak width).

When we compare the values of $\beta$ in Fig. 5 with those we can get from table 1 using Eq. 11 we find significant differences to most of the recent research works except the values of a study using Computational Fluid Dynamics by Lavante [Lavante].

The differences can have to fundamental reasons.

At first there could be systematic errors in the measurements, e.g. leakage in the set up. This can be excluded here, because the calibrations were done in very different experimental set ups mounted and remounted again and again[6]. Also the reference used for the calibrations were different and do not correlate with the peaks. A third problem (also described in [Lavante]) is an

[6] We spend a lot of effort to avoid any leakage effect, especially when small nozzles have to be calibrated.

unsteady effect of the flow which occurs depending on the pressure ratio across the nozzle. This can be excluded here, because we use ratios quite far in the stable region (normally $p_{ratio} < 0,1$) for our nozzle calibrations

The second reason can be systematic deviation in the geometry. Here we have up to now no direct proof, because we talk about calibrations done in the past and nobody cares about the conformity of the nozzle geometry to the specification at that time. But it is interesting to ask for the relations between our nozzle parameters and the geometry.

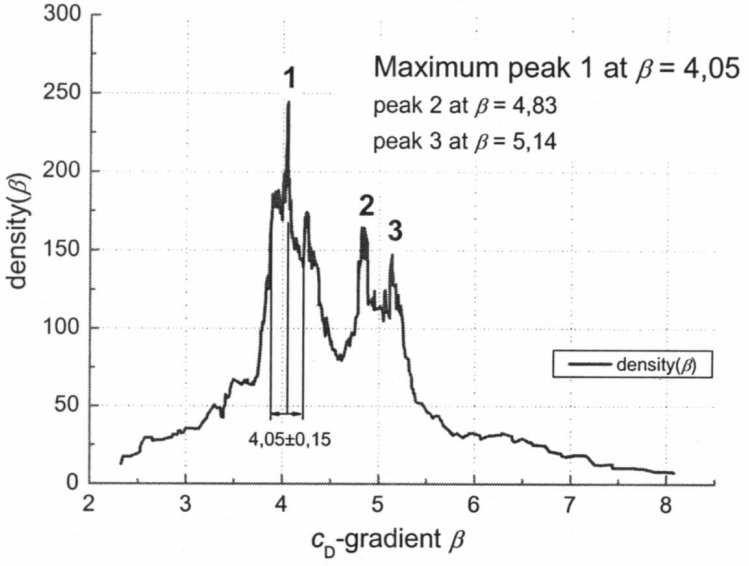


Fig. 6: Density of $c_D$-gradient $\beta$. The curve is determined from data set in Fig. 5 using Eq. 14 for the numeric density (with $m$ = 13). There can be obtained a sharp maximum peak (1) at $\beta$ = 4,05 with a small side peak and two secondary peaks (2 and 3 at $\beta$ =4,83 and 5,14). The maximum numeric density at $\beta$ = 4,05 is equivalent to the maximum probability density, therefore it is reasonable to chose this $\beta$ - value as the best estimation. Any kind of mean or median would not be helpful due to the very high asymmetry of the distribution and the fact, that we have here several subsets of $\beta$ which are statistical significant different (see also Fig. 4 for the uncertainties of $\beta$).
The variation of $\beta$ with ±0,15 (used as the $2\sigma$ – value) is a rough estimation from the peak width.

Relations of discharge coefficient $c_D$ to the geometry of nozzle

To explain the relations between the geometry of nozzle and our two parameters a and $\beta$ we refer to the theoretical studies of Hall and Geropp [Hall] [Geropp].

Hall [Hall] calculated the curvature of isotache in the core flow due to the 2-dimensionally flow in the nozzle entrance. He ignored any boundary layer, so his solution is valid for Eq. 13 at infinite high Reynolds numbers and express the parameter $a$. The solution depends only on the curvature radius $R$[7] of the nozzle and the isentropic exponent $\kappa$ of the gas:

Eq. 15 $$c_{D,inf,Hall} = a_{Hall} = 1 - \sum_{i=2}^{4} (-1)^i \frac{H_i}{R^i}$$

Eq. 16 $$H_2 = \frac{(\kappa + 1)}{386 \cdot R^2}$$

[7] Note that Hall used in his publication the half throat diameter $h = d/2$ as length scale for normalisation. The equations are transformed here to use always $d$ for reasons of consistent.

$$H_3 = \frac{(\kappa+1)(8\kappa+21)}{36864 \cdot R^3}$$

$$H_4 = \frac{(\kappa+1)(754\kappa^2+1971\kappa+2007)}{8847360 \cdot R^4}$$

For the practical values of $\kappa$ which can be between 1,2 (e.g. higher hydrocarbons) and 1,67 (one-atomic gases like helium, argon ect.) the dependence on $\kappa$ is nearly linear for a given curvature radius $R$:

Eq. 17 $a_{Hall} \approx 0.999425 - 5.62 \cdot 10^{-4} \cdot \kappa$ at $R = 2$.

The deviation from linearity is less than $10^{-6}$ (absolute). Eq. 17 shows additionally that the effect of $\kappa$ to the value of $a_{Hall}$ is small.

The solution for $R = 2$ und $\kappa = 1{,}4$ (air) is $a_{Hall} = 0{,}9986$. As we have no direct proof of this values except the results of table 1 we assume

Eq. 18 $a = 0{,}9985 \pm 0{,}0005$

as a good estimation which covers the most relevant experimental values inclusive any dependence on gas quality.

The other study of Geropp [Geropp] ignores vice versa the curvature of isotache in the core flow and gives a solution of the Prandtl-equation for the boundary layer. This means we will have a solution of Eq. 13 with $a = 1$ (no curvature of isotache):

Eq. 19 $$c_D = 1 - \frac{\beta}{\sqrt{Re}}$$

It is to be seen that the $c_D$-gradient $\beta$ is directly connected to the development of boundary layer thickness. It can be also called a speed factor of boundary layer development. Geropp found the solution depending only on the curvature radius $R$ of the nozzle and the isentropic exponent $\kappa$ of the gas:

Eq. 20 $$c_{D,Geropp} = 1 - \frac{G(\kappa) \cdot R^{0.25}}{\sqrt{Re}}$$

Eq. 21 $$G(\kappa) = 2 \cdot 8^{0.25} \left(\frac{\kappa+1}{2}\right)^{0.25} \left(3 \cdot \sqrt{2} - 2 \cdot \sqrt{3} + \frac{\kappa-1}{\kappa+1} \cdot \frac{8-3 \cdot \sqrt{6}}{\sqrt{3}}\right).$$

The Geropp-factor $G(\kappa)$ is also very close to linearity in the interesting region of $\kappa = 1{,}2 \ldots 1{,}67$:

Eq. 22 $G(\kappa) \approx 1.8956 + 0.7580 \cdot \kappa$

with deviation less than 0,006 (absolute).

Comparing Eq. 19 with Eq. 20 we get:

Eq. 23 $\beta = G(\kappa) \cdot R^{0.25}$.

The value of Geropp factor using Eq. 21 results

Eq. 24 $G = 2{,}962$ at $\kappa = 1{,}4$

what leads to

Eq. 25 $\beta_{Geropp} = 3.522$ at $R = 2$.

This value for $\beta$ is close to the recent experimental works (table 1) but significant different from our estimation $\beta = 4{,}05$ and the CFD-result of Lavante [Lavante] with $\beta = 4$.

This difference between theory and experimental results is also clear to be seen if we use Fig. 6 and transform it to the curvature radius using Eq. 23. In Fig. 7 the results are given for two cases. First (blue line) with the Geropp-factor $G = 2{,}96$ originally calculated by Geropp. In this case the maximum peak 1 is far away from the specification of the nozzle. More than 90 % of all nozzles should have a significant larger curvature radius than specified! The second (red) curve is

calculated in the way that the maximum peak is at $R$ =2. For this we have to use a Geropp-factor of $G$ = 3,4.

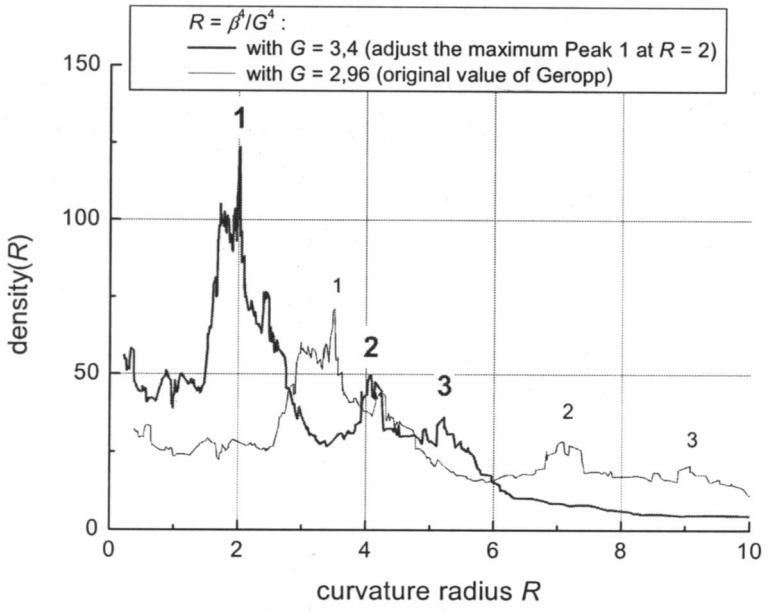


Fig. 7: Density of curvature radius $R$ ($R$ is determined from data of $\beta$ in Fig. 6 using the relation $R = \beta^4/G^4$, see also Eq. 23). There are two curves. One (blue) was calculated with application of the value $G$ = 2,96 original calculated by Geropp [Geropp] for gas with isentropic exponent $\kappa$ = 1,4 (air) and the second (red) with $G$ = 3,4, which adjusts the maximum peak 1 to the value $R$ = 2 (see also Fig. 6, the numbering of peaks are the same here). All of the evaluated nozzles should have the curvature radius $R$ = 2 from the specification of design, therefore it is reasonable to assume the maximum peak at $R$ = 2. The secondary peaks 2 and 3 indicate systematic deviations from the ideal form in sets of nozzles out of the same production series.

The final result

With our empirical value for the $c_D$-gradient $\beta$ = 4,05 ±0,15 and the estimation of the parameter a = 0,9985 ±0,0005 using the calculation of Hall we get as final result for the $c_D$-curve of a sonic nozzle (using Eq. 13):

Eq. 26 $$c_D = 0{,}9985 - \frac{4{,}04}{\sqrt{Re}}$$

In Fig. 8 this curve is given in comparison with the curves of Hall/Geropp and of PTB 99 [PTB 99] (which is also very close to NRLM 99 [NRLM 99]). It is to be seen that the differences are obtainable especially at lower Reynolds numbers. In the region above $Re = 5 \cdot 10^5$ the differences are within the uncertainties of our new experimental curve. But also at the low region with Re = 1000 to 10000 the experimental results are not in contradiction. If we apply atmospheric air, a $Re$ = 1000 means throat diameter of about $d$ = 0,1 mm. An uncertainty of only 1 µm in measurement of throat diameter $d$ would lead to an uncertainty of 2 % of the $c_D$-value. This shows the problems of $c_D$-determination via the conventional way at low Reynolds numbers and the potencies of the new approach.

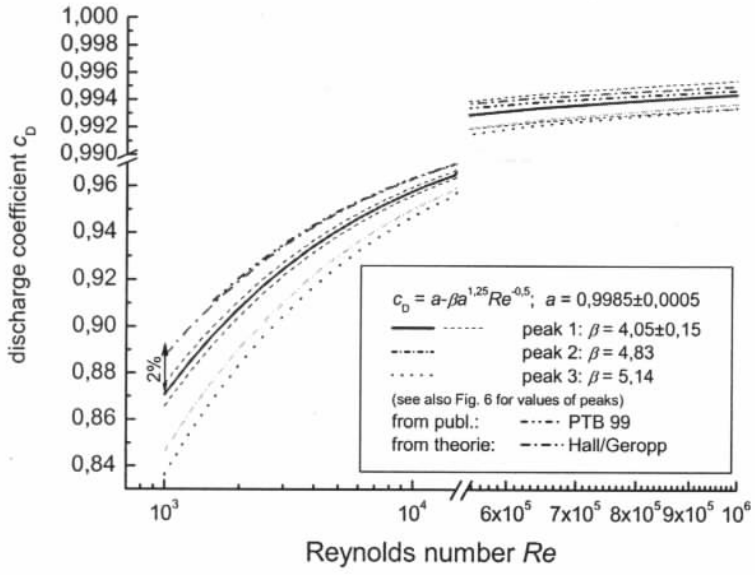


Fig. 8: Discharge coefficient based on $c_D = a - \beta a^{1,25} Re^{-0,5}$ (Eq. 13) with:
$a$ = 0,9985 ± 0,0005;
$\beta$ = 4,05 ± 0,15 (peak 1), $\beta$ = 4,83 (peak 2) and $\beta$ = 5,14 (peak 3).
For comparison, the curves of PTB 99 [PTB 99] and the theoretical curve Hall/Geropp [Hall] [Geropp] (see Eq. 25) are given. See also Fig. 6 for values of $\beta$.

Outlook to turbulent boundary layers

After determining the Eq. 13 for $c_D$ in dependence on $Re$ for laminar boundary layers it would be interesting to ask for possibilities to conclude from the laminar region to the turbulent one. The conventional formulation for the discharge coefficient in the turbulent region[8] is:

Eq. 27 $$c_D = a - \frac{b_{turb}}{\mathrm{Re}^{0.2}}$$

It is only a question of formalism to transform this equivalent to the way shown for laminar case into:

Eq. 28 $$c_D = \frac{a_d}{d^2} - \frac{b_{d,turb}}{d^{2.2}\,\mathrm{Re}^{0.2}} = C^{10} a_d - C^{11} b_d \frac{1}{\mathrm{Re}^{0.2}} \quad \text{with } C = \frac{1}{d^{0.2}}$$

With the same reasons and principles as above we come to:

Eq. 29 $$b_{turb} = \beta_{turb} \cdot a^{1.1} \text{ or } b_{d,turb} = \beta_{turb} \cdot a_d^{1.1}$$

and

Eq. 30 $$c_D = a - \frac{\beta_{turb} \cdot a^{1.1}}{\mathrm{Re}^{0.2}}$$

As mentioned above the parameter $\beta$ is also an expression for the speed of development of boundary layer thickness $\delta^*$. This development is quite good calculated for laminar as well as for turbulent boundary layers at plane plates (e.g. in [Albring]) which are one-dimensional and not accelerated:

Eq. 31 $$\delta^*_{lam,plate} = \frac{1.75}{\sqrt{\mathrm{Re}}} \text{ and } \delta^*_{turb,plate} = \frac{0.0463}{\mathrm{Re}^{0.2}}$$

[8] The parameter $a$ is independent to any boundary layer, therefore it is always the same.

For a first estimation we can now assume that the ratio between the non accelerated development to the accelerated one is the same for the laminar as well as for the turbulent case:

Eq. 32 $$\frac{\delta^*_{lam,plate}}{\beta_{lam}} = \frac{\delta^*_{turb,plate}}{\beta_{turb}}$$

This leads finally to the relation for an extrapolation from laminar to turbulent $c_D$:

Eq. 33 $$c_{D,turb} = a - \beta_{lam}\frac{0.0463}{1.75}a^{1.1}\mathrm{Re}^{-0.2}$$

The quality of this estimation is discussed in the accompanied paper [PTB 04/2] also in these proceedings.

## Conclusions

The question of the quality control of calibrations of very small nozzles down to throat diameters of 0,1 mm led to a new approach to conclude the discharge coefficient from flow rate measurements without any knowledge of throat diameter. In the centre of this approach is a new dimensionless parameter $\beta$ which characterises the gradient of the discharge coefficient in dependence on Reynolds number what is also equivalent to the speed of boundary layer development. The parameter $\beta$ is also strongly related to the geometry of nozzle and should be therefore a good tool for further theoretical and experimental studies. Further studies will be concentrated to these relations.

It has to be emphasising that the uncertainty of dimensionless results of different nozzles is much lower using $\beta$ especially at lower Reynolds numbers than the conventional way using the throat diameter. It allows also a reasonable conclusion from the behaviour of a nozzle in laminar region to the turbulent one.

## References


[Hall] Hall, G. W.: *Transonic flow in two-dimensial and axially-symmetric nozzles.* Qart. Journ. Mech. And Apllied Math., vol 15 (1962), pp 487 – 508

[Stratford 64] Stratford, B. S.: *The calculation of the discharge coefficient of profiled choked nozzles and the optimum profile for absolute air flow measurements.* Journ. Royal Aeronaut. Soc., April 1964, pp. 237 – 245

[Geropp] Geropp, D.: *Laminare Grenzschichten in ebenen und rotationssymmetrischen Lavaldüsen.* Forschungsbericht 71-90, DVLR 1971

[Arnberg 73] B.T.Arnberg, C.I.Britton and W.F.Seidl, *Discharge Coefficient Correlations for Circular Arc Venturi*

*Flow meters at Critical (Sonic) Flow*, ASME, 1973, No. 73-WA/FM-8.

[Arnberg 74] Arnberg, B. T.; Britton, C. L.; Seidl, W. F.: *Discharge coefficient correlations for circular-arc _enture flow meters at critical (sonic) flow.* Trans. ASME, Journ. Fluids Engineering, vol. 96 (1974), pp. 111 – 123

[Brain 77] T.J.S Brain and L.M Macdonald, *Evaluation of the performance of small scale critical flow venturis*

*using the NEL gravimetric gas flow standard test facility,* Fluid Flow Measurement in the mid

1970s, HMSO, Edinburgh, 1977, 103-125

[Brain 78] Brain, T. J. S.; Reid, J.: *Primary calibrations of critical flow Venturi*

*nozzles in high-pressure gas.* In: Flow Measurements of Fluids – FLOMEKO´78. H. H. Dijstelbergen, E. A. Spencer (eds.), North-Holland Publishing Company, 1979, pp. 55 – 64

[Aschi 78/79] Aschenbrenner, A.: *Ein Prüfstand für Großgaszähler mit überkritischen Düsen als Normalgeräte.* PTB-Bericht Me-24, PTB Braunschweig und Berlin, Oktober 1979, 36 Seiten.

[Ishibashi 94] Ishibashi, M.; Takamoto, M.; Watanabe, N.; Nakao, Y.: *Precise calibration of critical nozzles of various shapes at the Reynolds number of 0.8 – 2.5 x $10^5$.* In: Proceedings of the 7th International Conference on Flow Measurement, FLOMEKO´94, 23 – 17 June 1994, Glasgow/Scotland, paper 6.2, 14 pages

[Nakao] Nakao, S.; Yokoi, Y.; Takamoto, M.: Development of a calibration facility for small mass flow rates and the uncertainty of a sonic Venturi transfer standard. Flow Meas. Instrument., vol 7 (1996), pp. 77 – 83

[Miralles 98] B. T. Miralles, *On the experimental determination of the discharge coefficient of sonic nozzles for*

*Reynolds numbers from 4·$10^4$ to 2·$10^5$*, Flowmeco, 1998, 227-232

[PTB 99] Wendt, G.: *Einsetzbarkeit kritisch durchströmter Düsen mit Reynoldszahln kleiner 1x$10^5$ für die Durchflussmessung von Gasen.* PTB-MA-69, Braunschweig August 2000

[NRLM 99] Ishibashi, M.; Takamoto, M.: *Discharge coefficient of super accurate critical nozzles at pressurized condition.* In: Proceedings of the 4th International Symposium on Fluid Flow Measurement, 27 – 30 June 1999, Denver/Colorado, paper 6.3, 11 pages

[Park 2000] K.A Park, Y.M Choi, H.M Choi, T.S Cha, B.H Yoon: *CHARACTERISTICS OF SMALL SONIC NOZZLES.* In: Proceedings of the 10th International Conference on Flow Measurement, FLOMEKO 2000, 4 – 8 June 2000, Salvador/Brazil, paper F3, 7 pages

[Lavante] Lavante, E., Ishibashi, M. and Wendt, G., *Investigation of Flowfields in Small Sonic Venturi-Nozzles*, In Proceedings of 10th International Conference on Flow Measurement, FLOMEKO 2000, 4 – 8 June 2000, Salvador/Brazil

[Albring] Albring, W.: *Angewandte Strömungslehre*, Verlag Theodor Steinkopf, Dresden 1971

[PTB 04/2] Bodo Mickan, Rainer Kramer, Harald Dietrich, Ernst Lavante*, Manfred Jaeschke, Hans-Jürgen Hotze: *Measurements with sonic nozzles in high-pressure natural gas*, Also in this proceedings